

Polarity-reversal-producing phase transfer of hydrophilic silver nanoclusters capped by a hyperbranched polymer from water to nonpolar organic solvents

Fei Qu,^{1,2} Shuwen Niu,^{1,2} Jinmao You^{1,2,3}

¹Key Laboratory of Life-Organic Analysis, Qufu Normal University, Qufu 273165, Shandong, China

²Key Laboratory of Pharmaceutical Intermediates and Analysis of Natural Medicine, Qufu Normal University, Qufu 273165, Shandong, China

³Northwest Institute of Plateau Biology, Chinese Academy of Sciences, Xining 810001, China

Fei Qu and Shuwen Niu contributed equally to this work.

Correspondence to: F. Qu (E-mail: qufei3323@163.com) and J. You (E-mail: jmyou6304@163.com)

ABSTRACT: Hyperbranched poly(ethylene imine) (PEI)-capped Ag nanoclusters, synthesized starting from an aqueous environment, dispersed well in water and most polar organic solvents. However, with the addition of 1,4-dioxane, the PEI-capped Ag nanoclusters could be separated completely to obtain hydrophilic and hydrophobic Ag nanoclusters. Through this facile method, the successful phase transfer of PEI-capped Ag nanoclusters from the aqueous phase to the nonpolar organic phase, such as from water to carbon tetrachloride, chloroform, and methylene bichloride, was easily realized. The polarity reversal of Ag nanoclusters were considered to be associated with the conformational change of PEI on the basis of the hydrophobic methylene groups of polymer backbone facing the external side or internal side, and this polarity reversal was irreversible. Moreover, PEIs with higher molecular weights showed a higher efficiency of phase transfer of the Ag nanoclusters. © 2015 Wiley Periodicals, Inc. *J. Appl. Polym. Sci.* **2016**, *133*, 43206.

KEYWORDS: nanoparticles; nanowires and nanocrystals; phase behavior; polyelectrolytes; spectroscopy

Received 7 August 2015; accepted 9 November 2015

DOI: 10.1002/app.43206

INTRODUCTION

A combination of the virtues of chemistry with nanotechnology and various scaffold-encapsulated metal nanoclusters, in particular, gold and silver, have been developed as a new class of emitters that have drawn considerable attention because of possible applications in chemical analysis,^{1,2} catalysis,³ optics,^{4,5} and biology.^{6–8}

At present, various methods have been developed to synthesize metal nanoclusters^{9–11}; templates are usually used to cap metal nanoclusters because these small clusters aggregate easily to form larger nonfluorescent nanoparticles in aqueous media. Meanwhile, it is common to use nanoclusters in aqueous media in analysis and detection; these included metal ions,^{1,12} pH values,¹³ DNA,¹⁴ biological small molecules,^{15,16} and proteins.^{17,18} However, there has been little literature focusing on the application of nanoclusters in nonaqueous media. The reason was ascribed to two aspects: one was that metal nanoclusters are generally prepared from an aqueous environment, and the other is that most of the analytes reported exist in aqueous media.

However, some toxic compounds, bioactive molecules, and drugs are insoluble in water, for instance, Sudan red, steroid hormones, spironolactone, and misoprostol. Therefore, the study of the properties of nanoclusters in nonaqueous media is important for extending the range of applications. To date, several attempts have been made to develop protocols for the phase transfer of nanomaterials from the aqueous phase to the organic phase. These include the following:

1. The direct dispersal of water-soluble metal nanoclusters in polar organic solvents.¹⁹
2. The precipitation of metal nanoclusters and their redissolution in polar organic solvents.²⁰ The common shortcoming of the first two methods is that metal nanoclusters can only dissolve in polar organic solvents rather than in nonpolar organic solvents because there is no significant change in the polarity of these nanoclusters.
3. The modification of amphiphilic molecules on the surfaces of the metal nanoparticles. This modification can greatly vary the polarity of nanoclusters; this produces phase

Additional Supporting Information may be found in the online version of this article.

© 2015 Wiley Periodicals, Inc.

transfer from water to organic solvents. For instance, Dorokhin *et al.*²¹ reported the reversible phase transfer of quantum dots (QDs). First, trioctylphosphine oxide (TOPO)-stabilized CdSe/ZnS QDs were synthesized in an organic solvent, and then, ferrocene derivatives were modified on the surface of TOPO QDs to replace the TOPO. Subsequently, the addition of cyclodextrin produced the migration of the QDs to the water phase. Next, naphthalene or adamantane derivatives were effective in the replacement of ferrocene from the ring of cyclodextrin; this realized the reversible transfer of the QDs from the organic phase to water. Hence, these results suggested that the surface ligands determined the solubility of the nanoparticles. However, this method was relatively complicated and had limited practical application.

4. The addition of flexible ligands on the surfaces of the nanoparticles. This could make the phase transfer easier because of the conformational change of the ligands (hydrophilic or hydrophobic groups that switch between the inside and outside) in response to the polarity of the solvents. For example, silver nanoclusters capped by poly(methacrylic acid) (PMAA) were initially synthesized in an aqueous medium; when the clusters in aqueous solution were mixed with butanol, the hydrophobic methyl groups of PMAA were exposed to the solvent, and this made the composite silver nanoclusters prefer to move to the butanol phase.²² Therefore, it is a robust approach to use the conformational change of the templates for phase transfer.

In previous studies, we extensively examined the solvatochromism of hyperbranched poly(ethylene imine) (PEI)-capped silver nanoclusters, which were synthesized in aqueous solutions and could be well dispersed in water and most polar organic solvents.¹⁹ However, these clusters were insoluble in nonpolar organic solvents; this greatly limited the application of PEI-capped silver nanoclusters. In this assay, 1,4-dioxane was found to be a special solvent, and this could change the conformation of PEI and result in a complete separation of hydrophilic and hydrophobic Ag nanoclusters. Subsequently, a successful phase transfer could be easily realized for the PEI-capped Ag nanoclusters from the aqueous phase to the nonpolar organic phase, such as from water to carbon tetrachloride (CCl₄), chloroform (CHCl₃), and methylene dichloride (CH₂Cl₂). Hence, this strategy offered us a unique opportunity to study the optical properties of PEI-capped Ag nanoclusters in nonpolar organic solvents and would largely extend the application of PEI-capped Ag nanoclusters.

EXPERIMENTAL

Materials

Silver nitrate (AgNO₃), hyperbranched PEI [molecular weight (MW) = 600, 1800, 10,000, and 70,000], formaldehyde (35 wt %), water, methanol, ethanol, ethylene glycol (EG), isopropyl alcohol, *N,N*-dimethylformamide (DMF), dimethyl sulfoxide (DMSO), tetrahydrofuran (THF), 1,4-dioxane, *n*-butanol, CCl₄, CHCl₃, and CH₂Cl₂ were purchased from Aladdin (Shanghai, China). PEIs with MWs of 1300, 2000, 25,000, and 750,000 were purchased from Sigma-Aldrich (St. Louis, MO).

Methods

Fluorescence measurements were performed on a Hitachi F-7000 fluorescence spectrophotometer equipped with a quartz cell (1 × 1 cm²) in the emission mode. The slit widths were 10 and 10 nm for excitation and emission, respectively. The photomultiplier tube voltage was set at 400 V. The UV-visible absorption spectra were obtained on a Cary 300 Bio UV-visible spectrophotometer. The Fourier transform infrared (FTIR) spectra of the samples were analyzed by a WQF-520A FTIR spectrophotometer with KBr pellets. Transmission electron microscopy (TEM) and high-resolution transmission electron microscopy (HRTEM) images of the PEI-capped Ag nanoclusters were obtained with a Tecnai G2 F20 electron microscope. The X-ray diffraction (XRD) pattern was performed on a MiniFlex600 X-ray powder diffractometer.

Preparation of the PEI-Capped Ag Nanoclusters

Typically, certain amounts of PEIs with different MWs were first dissolved in deionized water by stirring for 2 min, and then, AgNO₃ was added and homogenized by stirring for 2 min. Subsequently, a formaldehyde solution (1 mol/L) was added with vigorous stirring. Because of the different MWs of PEI, the amounts of AgNO₃, PEI, and formaldehyde varied slightly. The detailed amounts of AgNO₃, PEI, and formaldehyde are shown in Table S1 (see Supporting Information). During this process, the color of the mixture changed from colorless to yellow; this indicated the formation of PEI-capped Ag nanoclusters (C1 clusters). The final solution was stored under ambient conditions for at least 4 days before further use.

Preparation of the C2 and C3 Clusters

Briefly, 50 μL of C1 clusters was diluted to 10 mL by 1,4-dioxane. A yellow precipitate was observed at the bottom of the solution, and the precipitate (C2 clusters) was separated from the solution. Subsequently, the supernatant was evaporated to obtain the C3 clusters.

Study of the Optical Properties of the C2 Clusters in 12 Different Solvents. The yellow precipitate mentioned previously (C2 clusters) was dispersed in 12 different solvents (10 mL), respectively; these included H₂O, DMSO, isopropyl alcohol, EG, methanol, CHCl₃, *n*-butanol, ethanol, DMF, CH₂Cl₂, THF, and CCl₄. Subsequently, the fluorescence spectra of these solutions were recorded with a fluorescence spectrophotometer.

Study of the Optical Properties of C3 Clusters in 12 Different Solvents. The supernatant of the C1 clusters in 1,4-dioxane was evaporated to obtain the C3 clusters. Then, these clusters were dispersed in 12 different solvents with a volume of 1 mL each; the solvents included H₂O, DMSO, isopropyl alcohol, EG, CHCl₃, *n*-butanol, ethanol, DMF, CH₂Cl₂, THF, and CCl₄. Finally, these solutions were analyzed with a fluorescence spectrophotometer.

Conversion Ratio of C1 to C2 and C3. Briefly, 200 μL of the C1 clusters was evaporated to a constant weight; then, another 200 μL of the C1 clusters was diluted to 40 mL by 1,4-dioxane to produce a yellow precipitate (C2 clusters), and then, these clusters were dried at 50–60°C to a constant weight. Subsequently, the supernatant was evaporated to obtain the C3

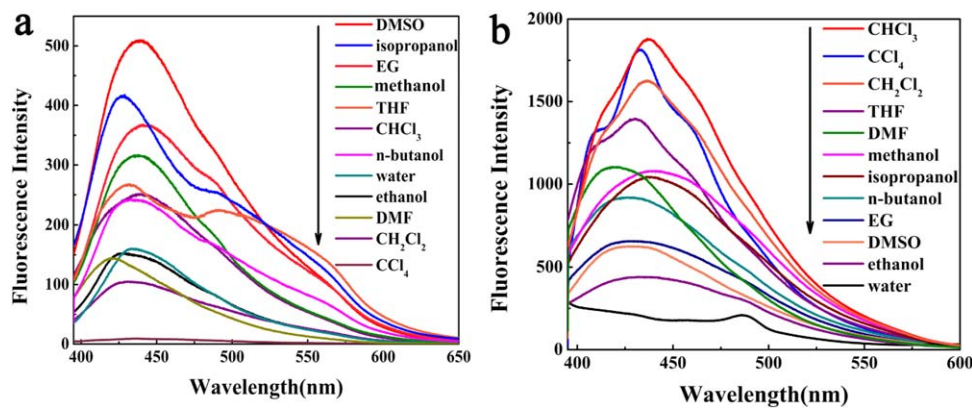


Figure 1. Fluorescence spectra of the (a) C2 and (b) C3 clusters in 12 different solvents. [Color figure can be viewed in the online issue, which is available at wileyonlinelibrary.com.]

clusters at a constant weight. Therefore, the conversion ratios of C1 to C2 and C1 to C3 were calculated through corresponding quality ratios, such as $W_{C2}/W_{C1} \times 100\%$ and $W_{C3}/W_{C1} \times 100\%$ in which W_{C1} , W_{C2} , and W_{C3} represented the quality of C1, C2, and C3 clusters.

Optimization of the Volume of 1,4-Dioxane for Complete Conversion. The experiment was carried out with the following steps: (1) 200 μL of the C1 clusters was diluted by 1,4-dioxane with different volumes (20, 30, 40, 60, and 70 mL); (2) all of the precipitates (C2 clusters) were separated from the solutions; (3) the corresponding supernatants were evaporated to obtain the C3 clusters, which were each dispersed in 4 mL of CCl_4 because of the good solubility of the C3 clusters in CCl_4 ; and (4) the fluorescence of these solutions was recorded.

RESULTS AND DISCUSSION

Synthesis of the PEI-Capped Ag Nanoclusters

In our previous work, silver nanoclusters capped by PEI with an MW of 10,000 were synthesized and constructed as multifunctional sensors.^{13,23} On the basis of a PEI-modified silver mirror reaction, PEIs with different MWs (600, 1300, 1800, 2000, 25,000, 70,000, and 750,000) were also used as templates to synthesize Ag nanoclusters, which possessed similar optical properties. For instance, the diluted solutions of these nanoclusters in water were nearly colorless under visible light and emitted intense blue fluorescence under a UV lamp; the characteristic absorption peaks of the Ag nanoclusters capped by PEIs with different MWs were located at 268 and 354 nm; these were attributed to the oligomeric silver species.^{24–26} The maximum fluorescence excitation and emission wavelengths were 375 and 455 nm, respectively, but the fluorescence intensities of these nanoclusters were different because of the various MWs of PEI (Figure S1, Supporting Information). Additionally, the characterizations, including XRD, FTIR spectroscopy, TEM and HRTEM, of these Ag nanoclusters are exhibited in Figures S2 and S3 (Supporting Information), respectively. The XRD pattern showed a broad diffraction peak located at a 2θ of about 38° because of the smaller Ag nanoclusters with nonmetallic properties.²⁷ The FTIR bands of the Ag nanoclusters appeared at 1657, 1468, and 1385 cm^{-1} ; these bands were attributed to the formation of imine after PEI reacted with

AgNO_3 .²⁸ In addition, all of these clusters displayed a spherical shape and uniform dispersal (Figure S3, Supporting Information), and the average particle diameters of the Ag nanoclusters capped by PEIs with MWs of 600, 1300, 1800, 2000, 10,000, 25,000, 70,000, and 750,000 were 2.95, 2.35, 4.4, 4.4, 1.95, 5.1, 1.95, and 2.25 nm, respectively.

Phase Transfer of the PEI-Capped Ag Nanoclusters from Water to Nonpolar Solvents

The solubility of the Ag nanoclusters was associated with that of template. PEI was dissolved well in water, most organic solvents, and some nonpolar organic solvents, except for CCl_4 . However, the PEI-capped Ag nanoclusters could only be dispersed in water and most polar organic solvents rather than nonpolar organic solvents. In this assay, 1,4-dioxane was found to be a special solvent, which could realize phase transfer of PEI-capped Ag nanoclusters from water to nonpolar organic solvents, such as CCl_4 , CHCl_3 , and CH_2Cl_2 . This phase transfer could be performed in three steps. First, the PEI-capped Ag nanoclusters (C1 clusters) were synthesized starting from water. Second, with the addition of 1,4-dioxane, a yellow precipitate (C2 clusters) was observed at the bottom of the solution. Third, after the separation of the precipitate, the supernatant was evaporated to obtain the C3 clusters. The conversion ratios of the C1 to C2 and C1 to C3 clusters were calculated through the corresponding quality ratios of $W_{C2}/W_{C1} \times 100\%$ (46.5%) and $W_{C3}/W_{C1} \times 100\%$ (55.8%), so the recovery of C1 was 102.3% [$(W_{C2} + W_{C3})/W_{C1} \times 100\%$]. This indicated that the C1 clusters were completely transformed to C2 and C3, and this revealed a high conversion efficiency for this strategy.

Because the optical properties of C1 clusters in polar organic solvents were studied previously,¹⁹ in this assay, the C2 and C3 clusters were investigated in deionized water and 11 different organic solvents, including methanol, ethanol, EG, isopropyl alcohol, DME, DMSO, THF, *n*-butanol, CCl_4 , CHCl_3 , and CH_2Cl_2 .

With Ag nanoclusters capped by PEI with a MW of 70,000 as an example, the results suggested that the C2 clusters were very soluble in H_2O , DMSO, isopropyl alcohol, EG, and methanol; partially soluble in CHCl_3 , *n*-butanol, ethanol, DMF, CH_2Cl_2 , and THF; and completely insoluble in CCl_4 . However, the solubility of the C3 clusters exhibited distinctive differences from

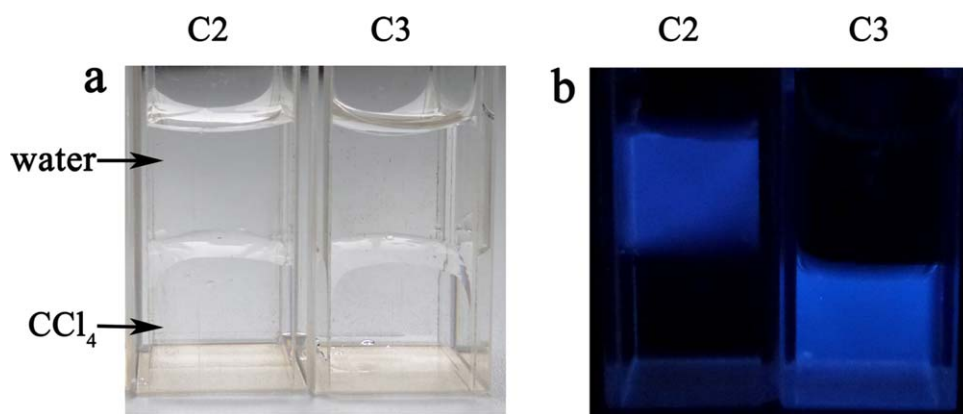


Figure 2. Photographs of the C2 clusters (left) and C3 clusters (right) dispersed in water and CCl_4 under (a) visible light and (b) 365-nm UV light. [Color figure can be viewed in the online issue, which is available at wileyonlinelibrary.com.]

those of the C2 clusters. The C3 clusters were well dispersed in CHCl_3 , CCl_4 , and CH_2Cl_2 ; partially soluble in THF, DMF, methanol, isopropyl alcohol, *n*-butanol, EG, DMSO, and ethanol; and completely insoluble in H_2O . The detailed solubilities of the C1, C2, and C3 clusters in various solvents are listed in Table S2 (see Supporting Information). According to these results, the fluorescence intensity exhibited regular variations, including a higher fluorescence in good solvents and a lower fluorescence in poor solvents (Figure 1). In addition, we also compared the absorption spectra of C1, C2, and C3 clusters, as shown in Figure S4 (Supporting Information), where the C1 and C2 clusters showed similar characteristic absorption features, which were located at 268 and 354 nm, and the C3 clusters displayed a distinctive absorption band around 300 nm; this was ascribed to the conformational change of the templates induced by solvents.

Furthermore, by virtue of the good solubility of C3 in CCl_4 , the fluorescence of the C3 clusters in CCl_4 was used to evaluate the optimal volume of 1,4-dioxane for complete conversion. As shown as Figure S5 (Supporting Information), with the addition of 40 mL of 1,4-dioxane, 200 μL of the C1 clusters could complete the conversion, so the optimal volume ratio of Ag nanoclusters to 1,4-dioxane was 1:200.

The efficient phase transfer of the fluorescent nanoclusters in the CCl_4 phase is also shown in the photographs in Figure 2. Under UV light at 365 nm, the CCl_4 phase (lower layer) containing C3 clusters and the water phase containing C2 clusters (upper layer) showed intense blue fluorescence; this suggested the good solubility of C3 clusters in the CCl_4 phase, whereas the C2 clusters remained in the water phase. The images indicated that under the assistance of 1,4-dioxane, the polarity of the Ag nanoclusters was obviously reversed, so the C3 clusters could be transferred to the organic phase where they remained luminescent, and no fluorescence could be obtained from the water phase. Therefore, the hydrophilic C2 clusters and hydrophobic C3 clusters could be separated completely, and the total phase transfer of the silver nanoclusters from the aqueous phase to the organic phase did not use a complex phase-transfer agent.

Additionally, the polarity reversal was also realized through 1,4-dioxane for Ag nanoclusters protected by PEIs with other MWs

(600, 1300, 1800, 2000, 10,000, 25,000, and 750,000). Through the evaporation of the supernatant of 1,4-dioxane after the separation of the precipitate, the C3 clusters capped by PEIs with different MWs were also soluble in CCl_4 , and they emitted blue fluorescence [Figure 3(a,b)]. The corresponding fluorescence spectra are shown in Figure 3(c); the C3 clusters capped by PEIs with higher MWs showed a stronger fluorescence than those capped by PEIs with lower MWs. Because of the fluorescence intensity in proportion to the amount of C3 clusters, PEIs with higher MWs easily produced the polarity reversal of the silver nanoclusters. Thus, to obtain greater amounts of hydrophobic Ag nanoclusters, Ag nanoclusters capped by PEIs with higher MWs should be used.

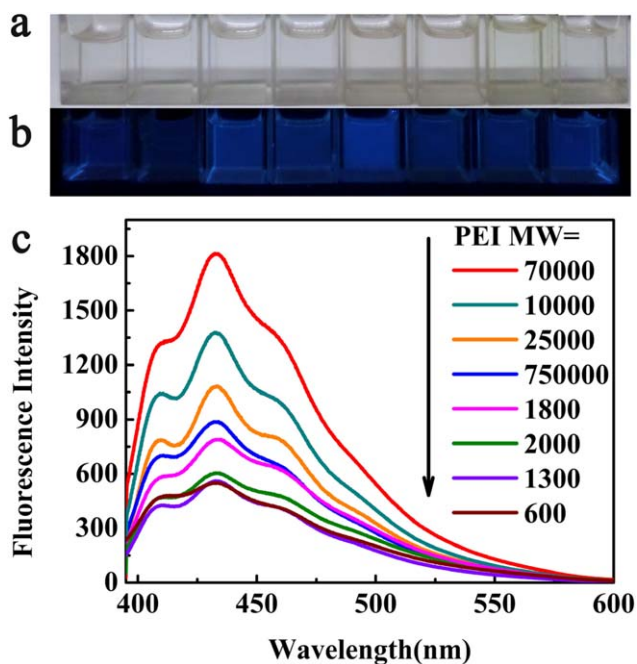


Figure 3. Photographs of the C3 clusters capped by PEIs with different MWs (600, 1300, 1800, 2000, 10,000, 25,000, 70,000, and 750,000 from left to right) in CCl_4 (a) under visible light and (b) under a UV lamp at 365 nm and (c) corresponding fluorescence spectra. [Color figure can be viewed in the online issue, which is available at wileyonlinelibrary.com.]

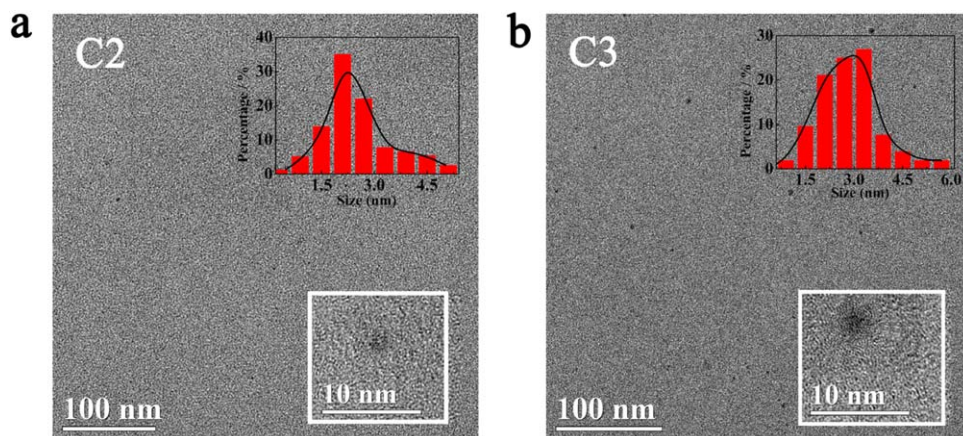


Figure 4. TEM and HRTEM images of the (a) C2 and (b) C3 clusters capped by PEI with an MW of 70,000. [Color figure can be viewed in the online issue, which is available at wileyonlinelibrary.com.]

Mechanism of the Polarity Reversal of the PEI-Capped Ag Nanoclusters

Previously, the successful phase transfer of PMAA–Ag nanoclusters from water to butanol was once reported by Ras *et al.*,²² in which the hydrophobic methyl groups of PMAA were exposed to butanol; this made the composite silver nanoclusters dissolve in the butanol phase. However, the transfer from water to the CCl_4 phase of the silver nanoclusters protected by PEI was not found because neither AgNO_3 nor PEI was soluble in CCl_4 . The major difference between the previous study and this study was that our protocol separated the hydrophilic and hydrophobic Ag nanoclusters completely through 1,4-dioxane. In addition, in a comparison of the TEM and HRTEM images of C1, C2, and C3 [Figure S3(g) and Figure 4], there were no obvious differences in the diameters and morphologies among these clusters, so we ascribed the polarity reversal to the conformational changes of PEI, and on the basis of the mechanism proposed by the previous literature,²² we rationalized the phase transfer as follows. PEI, as a hyperbranched polymer, contained primary, secondary, and tertiary amine groups; this efficiently chelated with the silver nucleus and stabilized these particles against flocculation by

the strong coulomb interactions. Because of the synthesis starting from water, it was reasonable to assume that some amino groups surrounded the silver nucleus, and some were directed toward aqueous solution; this resulted in the good solubility of the C1 clusters in water. In addition to the amino groups, the polymer backbone was also connected by hydrophobic methylene units; thus, when the nanoclusters were dispersed in 1,4-dioxane, the hydrophobic methylene groups facing the external side of the nanodomains were easily accessible to 1,4-dioxane molecules. This led to hydrophobic C3 clusters, which preferred to go to the nonpolar organic solvents. However, the flexibility of the PEI backbone was limited, and some of methylene groups still faced the internal side of the nanodomains (amino groups outside), so the hydrophilic C2 clusters readily formed as a precipitate. The polarity-reversing process of silver nanoclusters on the basis of the conformational change of PEI is displayed in Figure 5. Additionally, the chains of the polymer kept them further apart, and this reduced the forces of attraction between them and made the material more flexible, so the PEIs with higher MWs exhibited a higher efficiency of phase transfer of silver nanoclusters (Figure 3). Most importantly, the conformational change of

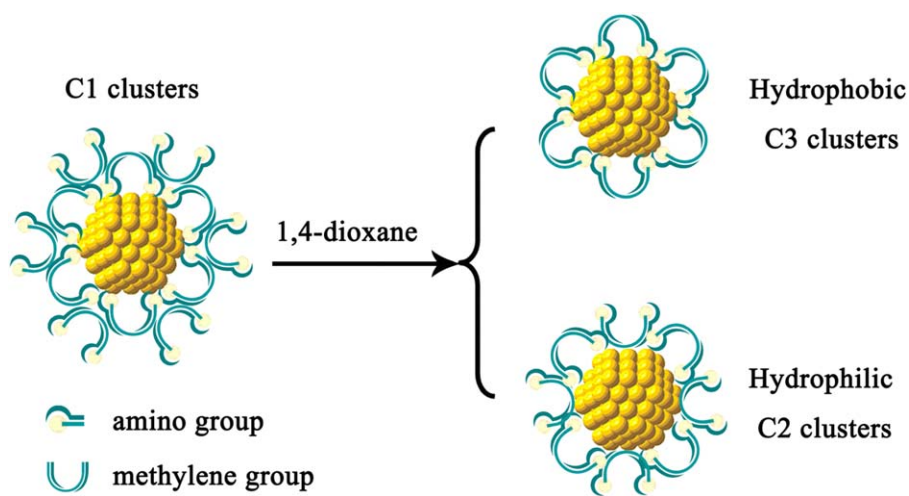


Figure 5. Polarity reversal of the silver nanoclusters based on the conformational change in PEI. [Color figure can be viewed in the online issue, which is available at wileyonlinelibrary.com.]

PEI was irreversible, and this will lead to different applications for the C2 and C3 clusters.

CONCLUSIONS

In this assay, with the assistance of 1,4-dioxane, Ag nanoclusters capped by PEIs with different MWs (600, 1300, 1800, 2000, 25,000, 70,000, and 750,000), as good water-soluble nanomaterials, were successfully transferred from water to nonpolar organic solvents, such as CCl₄, CHCl₃, and CH₂Cl₂. Moreover, the phase transfer allowed a facile process to separate the hydrophilic and hydrophobic silver nanoclusters, and both of them maintained their luminescence, where the flexible conformation change of PEI played a vital role. It is also hoped that this work will shed some light on the optical properties of metal clusters and expand the application of Ag nanoclusters in nonaqueous analysis and detection.

ACKNOWLEDGMENTS

This work was supported by the National Natural Science Foundation of China through the Youth Fund Project (contract grant number 21405093) and by the Scientific Research Foundation of Qufu Normal University (contract grant number BSQD20130117).

REFERENCES

1. Sun, J.; Yang, F.; Zhao, D. R.; Yang, X. *Anal. Chem.* **2014**, *86*, 7883.
2. Yuan, Z. Q.; Cai, N.; Du, Y.; He, Y.; Yeung, E. S. *Anal. Chem.* **2014**, *86*, 419.
3. Qian, H. F.; Jiang, D. E.; Li, G.; Gayathri, C.; Das, A.; Gil, R. R.; Jin, R. C. *J. Am. Chem. Soc.* **2012**, *134*, 16159.
4. Chakraborty, P. *J. Mater. Sci.* **1998**, *33*, 2235.
5. Selvan, S. T.; Hayakawa, T.; Nogami, M.; Kobayashi, Y.; Liz-Marzan, L. M.; Hamanaka, Y.; Nakamura, A. *J. Phys. Chem. B* **2002**, *106*, 10157.
6. Collins, J. A.; Xirouchaki, C.; Palmer, R. E.; Heath, J. K.; Jones, C. H. *Appl. Surf. Sci.* **2004**, *226*, 197.
7. Luo, Z. T.; Zheng, K. Y.; Xie, J. P. *Chem. Commun.* **2014**, *50*, 5143.
8. Liu, X. Q.; Wang, F. A.; Aizen, R.; Yehezkeli, O.; Willner, I. *J. Am. Chem. Soc.* **2013**, *135*, 11832.
9. Yuan, X.; Luo, Z. T.; Zhang, Q. B.; Zhang, X. H.; Zheng, Y. G.; Lee, J. Y.; Xie, J. P. *ACS Nano* **2011**, *5*, 8800.
10. Díez, I.; Ras, R. H. A. *Nanoscale* **2011**, *3*, 1963.
11. Petty, J. T.; Zheng, J.; Hud, N. V.; Dickson, R. M. *J. Am. Chem. Soc.* **2004**, *126*, 5207.
12. Liu, J.; Ren, X. L.; Meng, X. W.; Fang, Z.; Tang, F. Q. *Nanoscale* **2013**, *5*, 10022.
13. Qu, F.; Li, N. B.; Luo, H. Q. *Langmuir* **2013**, *29*, 1199.
14. Obliosca, J. M.; Liua, C.; Yeh, H. C. *Nanoscale* **2013**, *5*, 8443.
15. Shang, L.; Dong, S. J. *Biosens. Bioelectron.* **2009**, *24*, 1569.
16. Han, B. Y.; Wang, E. K. *Biosens. Bioelectron.* **2011**, *26*, 2585.
17. Chen, C. T.; Chen, W. J.; Liu, C. Z.; Chang, L. Y.; Chen, Y. C. *Chem. Commun.* **2009**, *45*, 7515.
18. Sharma, J.; Yeh, H. C.; Yoo, H.; Werner, J. H.; Martinez, J. S. *Chem. Commun.* **2011**, *47*, 2294.
19. Qu, F.; Dou, L. L.; Li, N. B.; Luo, H. Q. *J. Mater. Chem. C* **2013**, *1*, 4008.
20. Díez, I.; Pusa, M.; Kulmala, S.; Jiang, H.; Walther, A.; Goldmann, A. S.; Müller, A. H. E.; Ikkala, O.; Ras, R. H. A. *Angew. Chem. Int. Ed.* **2009**, *48*, 2122.
21. Dorokhin, D.; Tomczak, N.; Han, M. Y.; Reinhoudt, D. N.; Velders, A. H.; Vancso, G. J. *ACS Nano* **2009**, *3*, 661.
22. Díez, I.; Jiang, H.; Ras, R. H. A. *ChemPhysChem.* **2010**, *11*, 3100.
23. Qu, F.; Li, N. B.; Luo, H. Q. *Anal. Chem.* **2012**, *84*, 10373.
24. Ershov, B. G.; Janata, E.; Henglein, A.; Fojtik, A. *J. Phys. Chem.* **1993**, *97*, 4589.
25. Ershov, B. G. *J. Phys. Chem. B* **1998**, *102*, 10663.
26. Linnert, T.; Mulvaney, P.; Henglein, A.; Weller, H. *J. Am. Chem. Soc.* **1990**, *112*, 4657.
27. Rao, T. U. B.; Nataraju, B.; Pradeep, T. *J. Am. Chem. Soc.* **2010**, *132*, 16304.
28. Tang, Y. R.; Zhang, Y.; Su, Y. Y.; Lv, Y. *Talanta* **2013**, *115*, 830.